Anti-Stokes Generation in Trapped Filaments of Light

C. A. SACCHI* AND C. H. TOWNES†
Massachusetts Institute of Technology, Cambridge, Massachusetts‡
AND
J. R. LIFSITZ
National Aeronautics and Space Administration, Electronics Research Center, Cambridge, Massachusetts

(Received 27 May 1968)

The angles of emission and frequency shifts of anti-Stokes radiation from small-scale trapped filaments of intense laser light in a number of liquids are examined and interpreted theoretically. For a given order of vibrational anti-Stokes radiation, a plot of angle of emission versus frequency resembles sections of nested parabolas which open towards higher frequencies, with apices a few tens of wave numbers below the unshifted anti-Stokes frequency, and very little intensity extending above this unshifted frequency. Various modulation mechanisms which smear out the Stokes and anti-Stokes frequencies are discussed, as well as the wave-vector matching conditions which appear to produce the angular distribution of radiation. Relatively simple approximations predict that the maximum extent towards lower frequencies of parabolas associated with the first anti-Stokes is one-half the vibrational frequency. The second and third anti-Stokes can extend twice and three times as far, respectively. In addition, a single set of parabolas is predicted for the first anti-Stokes radiation, but two sets for the second and third anti-Stokes. Theoretical expectations seem to agree reasonably well with observations.

I. INTRODUCTION

THE stimulated Raman radiation produced by high-power laser light in liquids reveals interesting spectral and directional properties. Unusual frequency broadening of the spectra was first reported by Stoicheff.[1] Garmire[2] introduced the distinction between two classes of radiation and showed that class I is generated by volume phase matching of the interacting waves, while class II, the type usually observed, is generated in filaments of laser light less than 0.2 mm in diameter and couples with Stokes radiation near the forward direction. Subsequently, Chiao *et al.*[3] found that the most intense Stokes light is produced in filaments of self-trapped laser light with a very small diameter (typically a few microns) and pointed out the importance of the change of index of refraction of the filaments on the directional and spectral properties of the anti-Stokes (AS) radiation. Shimoda[4] has also considered the effects of small filaments on the stimulated AS radiation. Here we suggest a model for the generation of the AS radiation of class II which leads to a prediction of the spectral and angular properties of this radiation consistent with the experimental results.

II. EXPERIMENTAL RESULTS

While the Stokes component of the Raman radiation generated in filaments of laser light is almost all trapped,[3] most of the AS component is not trapped, but emerges from the filaments with an angular distribution with respect to the axis of the filaments. We have reexamined the angular and spectral properties of this emitted AS radiation, studying the spectrum of the far field pattern. Since previous experiments[1,2] indicated a dependence of the frequency broadening of the Raman spectra on the multimode laser operation, an effort was made to carry out experiments with a single-mode ruby laser, in order to simplify the theoretical interpretation.

A ruby laser Q-switched with phthalocyanine and with a power of $\sim$50 MW/cm^2 was employed in the arrangement shown by Fig. 1. Fabry-Perot interferograms with a resolution of 10^{-2} cm^{-1} indicated that the laser was operating primarily in a single longitudinal mode. However, one cannot rule out the possibility that a small fraction of the laser energy was produced in very short pulses, which would give a continuous or broad spectrum rather than a series of simple modes of detectable intensity. Such pulses, furthermore, could have been of importance in producing nonlinear effects because of their possible high-peak intensity. Except for this type of possibility, the laser was clearly operating in a single mode.

The prisms A, B, C of Fig. 1 provide a long ($\sim$8 m) path for the beam before entering the cell containing the liquid, allowing sufficient time delay to prevent reamplification of the back-scattered Brillouin radiation which would produce a multiple frequency beam.[5] The lens L_1 (f=1.5 m) collimates the beam and lens L_2

* NATO—Italian CNR Fellow, now at Istituto di Fisica, Politecnico Milan, Italy.

† Now at the University of California, Berkeley, Calif.

‡ Work supported by the National Aeronautics and Space Administration and Air Force Cambridge Research Laboratories.

[1] B. P. Stoicheff, in *Quantum Electronics and Coherent Light*, edited by C. H. Townes and P. A. Miles (Academic Press Inc., New York, 1964), p. 306.

[2] E. Garmire, in *Physics of Quantum Electronics*, edited by P. L. Kelley, B. Lax, and P. E. Tannenwald (McGraw-Hill Book Co., New York, 1966), p. 167; also, thesis, Massachusetts Institute of Technology, 1965 (unpublished).

[3] R. Y. Chiao, M. A. Johnson, S. Krinsky, H. A. Smith, C. H. Townes, and E. Garmire, IEEE J. Quant. Electron. QE-2, 467 (1966).

[4] K. Shimoda, Japan J. Appl. Phys. 5, 615 (1966).

[5] E. Garmire and C. H. Townes, Appl. Phys. Letters 5, 84 (1964).

images the cones of emission of the AS radiation on the slit of a spectrograph to record the angular-versus-frequency distribution of this radiation. The cell was 12 cm long and the liquids employed were carbon disulfide, benzene, toluene, and nitrobenzene. Figure 2 gives a few examples of the observed spectra; more examples can be found in Ref. 2.

While power levels for the two cases could not be directly compared, the angular and spectral properties observed under the single-mode operation described here were found to be essentially the same as obtained by Garmire[2] under multimode operation. These properties can be briefly summarized as follows:

1. Under normally strong excitation, the first three orders of the AS radiation are frequency broadened respectively by about 12, 25, and 50% of the molecular vibrational frequency in all liquids examined except nitrobenzene. The latter shows a frequency broadening which is considerably smaller.
2. The spectra are predominantly shifted to the low-frequency side.
3. The second and third AS radiations exhibit, in general, two distinct cones of emission.
4. A display of radiation angle versus frequency for these spectra often presents well-defined curves, approximately parabolic in shape, and can be described as a superposition of parabolas of the form

$$\phi_i'^2 = a_{0i} + a_{1i}\omega_{Ri}.$$

Here a_{0i} and a_{1i} are variable parameters of a family of curves, ϕ_i' is the half-angle of the AS emission cone of order i, and ω_{Ri} is the shift from the normal AS frequency given by the sum of laser plus molecular vibration frequencies.

The spectral properties of the Stokes radiation involved in the AS generation,[6] first examined by Stoicheff,[1] have recently been studied in some detail.[7–9] The Stokes light is predominantly generated and trapped in filaments of small diameter (a few microns), and this component of the Stokes radiation exhibits a very broad spectrum generally more intense on the low frequency side. A pattern of discrete frequencies has been detected in the broadening of both the Stokes and the laser light in filaments.[9–10]

There is a significant correlation between the spectral properties of Stokes and AS radiation. Near-field observations at the AS frequency reveal the presence of trapped radiation with essentially the same spectral properties as the Stokes radiation. The broadening of the AS radiation which is not trapped is also found to be closely connected with occurrence of Stokes broadening. The magnitude of broadening of Stokes and AS radiation is correlated from shot to shot of the ruby laser, and is comparable in size. Furthermore, observations of the spectra of single filaments reveal that while pure nitrobenzene does not produce significant frequency broadening, in a solution of nitrobenzene and carbon disulfide the Stokes lines of nitrobenzene exhibit a broadening which depends on the relative concentration of the two liquids. Corresponding spectral characteristics, although with the broadening reduced in extent, is found in the far field pattern of the AS lines shown in Fig. 3. This observation also demonstrates the importance of the molecular rotational time in the processes which produce frequency broadening.[7]

It is also important to consider the spectral properties of the laser light within the filaments. This is frequently broadened, but never as strongly as the Raman components, and there is characteristically considerable intensity at the frequency of the original laser beam. This is presumably because light from the main laser beam is continuously entering the filament along its length, hence a considerable amount of light at the "pure" laser frequency is always present in the filaments together with light trapped before and already converted to other frequencies by the processes mentioned below. This trapped laser light may exhibit frequency broadening somewhat similar to that of the Stokes light but considerably reduced in strength relative to the unmodified laser light.

III. MECHANISMS WHICH BROADEN THE RAMAN SPECTRA

The following processes, of importance inside the filaments because of the intense electric field ($\sim 10^7$ V/cm) can affect the Raman scattering, and hence the

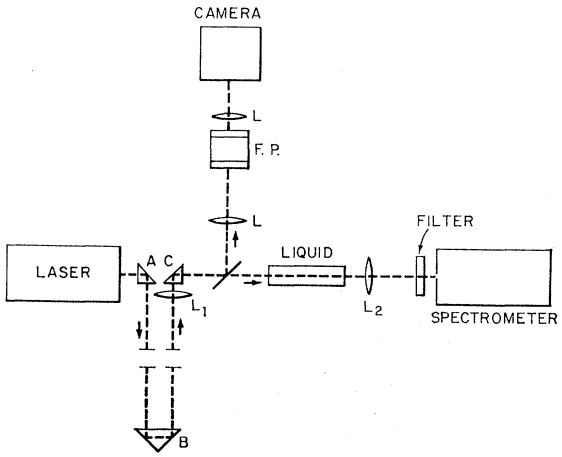

FIG. 1. Arrangement for observing frequency and angular distribution of stimulated Raman radiation.

[6] E. Garmire, F. Pandarese, and C. H. Townes, Phys. Rev. Letters 11, 160 (1963); R. Y. Chiao, E. Garmire, and C. H. Townes, in *Quantum Electronics and Coherent Light*, edited by C. H. Townes and P. A. Miles (Academic Press Inc., New York, 1964), p. 326.
[7] N. Bloembergen and P. Lallemend, Phys. Rev. Letters 16, 81 (1966).
[8] R. G. Brewer, Phys. Rev. Letters 19, 8 (1967).
[9] H. P. H. Grieneisen, J. R. Lifsitz, and C. A. Sacchi, Bull. Am. Phys. Soc. 12, 686 (1967); and (to be published).
[10] F. Shimizu, Phys. Rev. Letters 19, 1097 (1967).

properties of AS radiation:

1. Stimulated Rayleigh scattering due to molecular rotational motion.
2. Induced interaction between molecules.
3. Pulse distortion (self-steepening and phase modulation or pseudo-Doppler-shifts.[10–13]

The first and second processes may be directly involved in AS generation. Their influence is analytically expressed in the treatment done below. Included in mechanism 1 is the usual Rayleigh scattering associated with orientation of molecules against viscous forces, and also their pendular vibration in an intense optical field. The third process is perhaps the most important in producing the extreme frequency broadening of the trapped light and therefore of the Stokes or laser radiation, but it should have only an indirect influence on the properties of the AS radiation which is generated in filaments but is not trapped. The analytical treatment done below, which takes account of the third process in an indirect way, is adequate to derive the wave-vector relations that we use to explain the properties of the untrapped AS radiation.

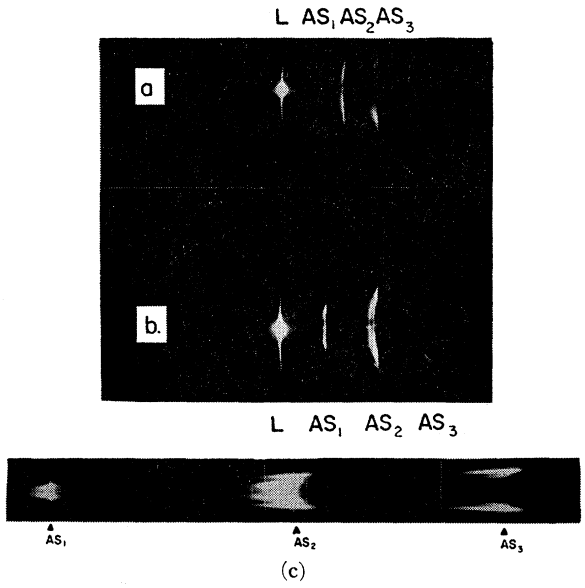

(c)

FIG. 2. Typical patterns of AS-radiation, with frequency increasing from left to right, and angle of the radiation measured up or down from the symmetry axis, which corresponds to the direction of the laser light. Frequency separation between AS orders (AS_1, AS_2, AS_3) corresponds to the molecular vibrational frequency of a few hundred wave numbers. Maximum angle deviations in these figures are about $\pm 5°$. Spectra shown are for (a) carbon disulfide, (b) benzene, and (c) toluene. Because of varying spectral sensitivity of the film (Polaroid 57) and the filters used (Corning glass 4-97), the pictures do not accurately represent the relative intensities of the laser frequency and different AS orders.

[11] R. J. Joenck and R. Landauer, Phys. Letters **24A**, 228 (1967).
[12] F. DeMartini, C. H. Townes, T. K. Gustafson, and P. L. Kelley, Phys. Rev. **164**, 313 (1967).
[13] A. Cheung, R. Y. Chiao, D. L. Rank, and C. H. Townes, Phys. Rev. Letters **20**, 786 (1968).

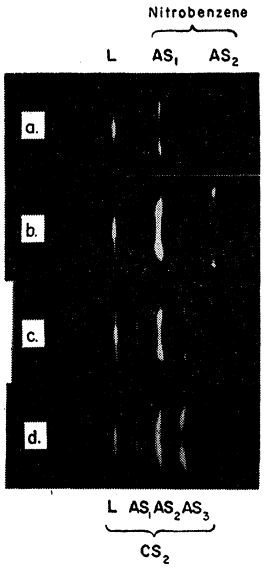

FIG. 3. Examples of AS-spectra in a mixture of nitrobenzene and carbon disulfide. The frequency broadening of the AS lines depends on the relative concentration of the two liquids. (a) Pure nitrobenzene, (b) mixture with 40% (volume) CS_2, (c) mixture with 45% (volume) CS_2, (d) mixture with 66% (volume) CS_2.

IV. MODULATION DUE TO RAYLEIGH SCATTERING

Since the molecular orientational Kerr effect is considered to be the principal trapping mechanism,[14] it is natural to investigate the influence of the Kerr effect on the Raman effect. Consider a symmetric top molecule for simplicity, with principal polarizabilities α_3 and α_1, where α_3 is the polarizability along the molecular axis. Assume the axis makes an angle Θ with the electric field $\mathbf{E}$, and $\alpha_3 > \alpha_1$. The potential energy of a molecule, without interaction with other molecules, is

$$W = -\tfrac{1}{2}(\alpha_3-\alpha_1)E^2\langle\cos^2\Theta\rangle_\Theta - \tfrac{1}{2}\alpha_1 E^2, \qquad (1)$$

where the averaging is over the distribution of angles Θ. As a consequence, the force driving the vibration of the molecule is

$$F = -\partial W/\partial x = \tfrac{1}{2}(\partial\alpha/\partial x)(1+bs)E^2, \qquad (2)$$

where x is a vibrational coordinate of the molecule, and

$$\partial\alpha/\partial x = (\partial\alpha_1/\partial x) + \tfrac{1}{3}[\partial(\alpha_3-\alpha_1)/\partial x],$$

$$b = \frac{\partial(\alpha_3-\alpha_1)/\partial x}{\tfrac{1}{3}[\partial(\alpha_3-\alpha_1)/\partial x] + (\partial\alpha_1/\partial x)}.$$

$s = \langle\cos^2\Theta - \tfrac{1}{3}\rangle_\Theta$ is a function describing the degree of orientation of the molecules of the liquid in the electric field and satisfying the following equation[15]:

$$\dot{s} + (s/\tau) = AE^2, \qquad (3)$$

where τ is the relaxation time for the amount of orientation to decay to $1/e$ of its original value after E is suddenly made zero. The value of A when

$$(\alpha_3-\alpha_1)E^2/KT \ll 1$$

[14] R. G. Brewer, J. R. Lifsitz, E. Garmire, R. Y. Chiao, and C. H. Townes, Phys. Rev. **166**, 326 (1968).
[15] J. Frenkel, *Kinetic Theory of Liquids* (Dover Publications, Inc., New York, 1955).

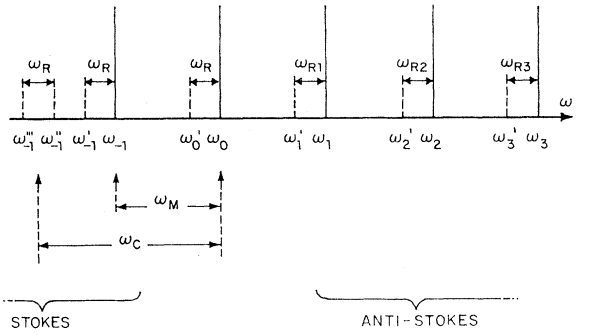

FIG. 4. Diagram of frequencies and symbols used for them. ω_0 is the original laser frequency, ω_{-1} the Stokes frequency shifted from ω_0 by exactly the molecular vibrational frequency ω_M. The quantities ω_1, ω_2, and ω_3 are the corresponding AS frequencies shifted by multiples of ω_M.

is

$$A=\tfrac{2}{45}(\alpha_3-\alpha_1)/KT\tau.$$

The equation for the vibration of the molecule of average orientation becomes

$$m\ddot{x}+R\dot{x}+h_0x=\tfrac{1}{2}(\partial\alpha/\partial x)(1+bs)E^2 \qquad (4)$$

and differs from the equation used in Ref. 6 by the term (bs), which describes the influence of the Kerr effect. Equation (3) is solved using two fields with a frequency difference ω_R in the range $\omega_R\tau\lesssim 1(\tau\simeq 10^{-9}-10^{-13}$ sec.). Then the generation of AS radiation is obtained[6] by solving Eq. (4) and calculating the rate of exchange of energy $P_{E'}$ between the resulting induced dipole moment $\mathfrak{y}$ and an AS field E', with

$$\mathfrak{y}=(\partial\alpha/\partial x)x(1+bs)\mathbf{E} \qquad (5)$$

and

$$P_{E'}=-\langle(d\mathfrak{y}/dt)\cdot\mathbf{E}'\rangle. \qquad (6)$$

To solve Eq. (3) for the molecular rotation and Eq. (4) for the molecular vibration, consider now the following two extreme cases for the spectral composition of the laser light in a filament:

(a) The laser light has a broad spectrum, similar in shape to that of the first Stokes spectrum, being broadened by the same processes.

(b) The laser light is essentially monochromatic. Although the actual spectrum may be more complicated than the simple superposition of these cases, nevertheless either one represents a reasonable approximation to certain observed cases, and each allows a fairly satisfactory description of observed AS radiation.

Case (a), which we consider first, corresponds to stimulated AS scattering due to the interaction between Stokes radiation and laser light which has been trapped in a filament for some distance and hence modulated in frequency. The modulation process may be mechanisms 1 or 2 listed above. However, it seems likely that the third mechanism, pulse distortion, will produce a much larger frequency broadening than successive stimulated Rayleigh scatterings. Pulse distortion is very effective in frequency broadening if there is some rapid intensity modulation initiated, for example, by either the presence of multiple modes in the laser or by the onset of Rayleigh scattering.[11] Pulse steepening contributes further to this process and to increase intensity towards lower frequencies. The various frequencies involved are indicated in Fig. 4, and hereafter a field strength E will be given the same subscripts and superscripts as its frequency. We assume that the fields are linearly polarized and parallel and are expressed in complex notation as

$$E_i=\tfrac{1}{2}[\mathcal{E}_i\exp[i(\mathbf{K}_i\cdot\mathbf{r}-\omega_it)]+\text{c.c.}];$$
$$\mathcal{E}_i=|E_i|\exp(i\phi_i).$$

The molecular rotational motion is driven at a frequency ω_R by forces proportional to $\mathbf{E}_0\cdot\mathbf{E}_0'$ and $\mathbf{E}_{-1}\cdot\mathbf{E}_{-1}'$, with $\omega_0-\omega_0'=\omega_{-1}-\omega_{-1}'=\omega_R$. With the phase-matching assumption

$$(\mathbf{K}_0-\mathbf{K}_0')\cdot\mathbf{r}+(\phi_0-\phi_0')=(\mathbf{K}_{-1}-\mathbf{K}_{-1}')\cdot\mathbf{r}+(\phi_{-1}-\phi_{-1}'), \qquad (7)$$

we obtain for s the solution

$$s=s_0+\tfrac{1}{2}[s_1'\exp(i\omega_Rt)+\text{c.c.}]=s_0+s_1. \qquad (8)$$

Here

$$s_0=\tfrac{1}{45}[(\alpha_3-\alpha_1)/KT](|E_0|^2+|E_0'|^2+|E_{-1}|^2+|E_{-1}'|^2), \qquad (9)$$

$$s_1'=\frac{2}{45}\frac{\alpha_3-\alpha_1}{KT}\frac{|E_0||E_0'|+|E_{-1}||E_{-1}'|}{[1+(\omega_R\tau)^2]^{1/2}}e^{-i\phi}, \qquad (10)$$

$$\phi=(\mathbf{K}_{-1}-\mathbf{K}_{-1}')\cdot\mathbf{r}+(\phi_{-1}-\phi_{-1}')+\tan^{-1}\omega_R\tau$$
$$=(\mathbf{K}_0-\mathbf{K}_0')\cdot\mathbf{r}+(\phi_0-\phi_0')+\tan^{-1}\omega_R\tau. \qquad (11)$$

Since the spectra of the laser and Stokes light have been assumed similar, we have also

$$|E_0'|/|E_0|=|E_{-1}'|/|E_{-1}|. \qquad (12)$$

Because of the relation (12) the force

$$F'=\tfrac{1}{2}\frac{\partial\alpha}{\partial x}(1+bs_0)E^2$$

with the terms $(\mathbf{E}_0\cdot\mathbf{E}_{-1})$, $(\mathbf{E}_0'\cdot\mathbf{E}_{-1}')$ and the force $F''=\tfrac{1}{2}(\partial\alpha/\partial x)bs_1E^2$ with the terms $(\mathbf{E}_0\cdot\mathbf{E}_{-1}')$ and $(\mathbf{E}_0'\cdot\mathbf{E}_{-1})$, drive the molecular vibration with the same phase and the solution of (4) is

$$x=\tfrac{1}{2}(X\exp\{i[\omega_Mt-(\mathbf{K}_0-\mathbf{K}_{-1})\cdot\mathbf{r}]\}+\text{c.c.}). \qquad (13)$$

Here

$$X=X_0\exp[-i(\phi_0-\phi_{-1}+\tfrac{1}{2}\pi)],$$
$$X_0=\tfrac{1}{2}(\partial\alpha/\partial x)(\omega_MR)^{-1}\{(1+bs_0)\times(|E_0||E_{-1}|+|E_0'||E_{-1}'|)+b|s_1'||E_0||E_{-1}'|[1+(\omega_R\tau)^2]^{-1/2}\}.$$

The second case, (b), which is to be considered now, corresponds to stimulated AS scattering due to Stokes light already produced and broadened in frequency

inside a filament and "fresh" laser light flowing into the filament from the main beam. The experimental evidence for a maximum intensity of the Stokes light on the low-frequency side at a shift ω_c from ω_0 (Fig. 4) suggests that the fields E_{-1}'' and E_{-1}''' may be the most important in driving the molecular rotations. In this case F' gives for x a solution similar to (13) but with

$$X_0=\tfrac{1}{2}(\partial\alpha/\partial x)\,(\omega_M R)^{-1}(1+bs_0)\,|\,E_0\,|\,|\,E_{-1}\,|\,, \quad (14)$$

and F'' gives

$$x=\tfrac{1}{2}\{X'\exp(i[\omega_M t-(\mathbf{K}_0-\mathbf{K}_{-1}'-\mathbf{K}_{-1}''+\mathbf{K}_{-1}''')\cdot\mathbf{r}]) +\text{c.c.}\}, \quad (15)$$

with

$$X'=X_0'\exp[-i(\phi_0-\phi_{-1}'-\phi_{-1}''+\phi_{-1}''' - \tan^{-1}\omega_R\tau+\tfrac{1}{2}\pi)],$$

$$X_0'=\tfrac{1}{4}(\partial\alpha/\partial x)\,(\omega_M R)^{-1}b\,|\,s_1'\,|\,|\,E_0\,|\,|\,E_{-1}'\,|\,.$$

We consider now the relations (5) and (6). The first term of the varying dipole moment expression (5),

$$\mathfrak{y}'=(\partial\alpha/\partial x)\times\mathbf{E}, \quad (16)$$

may produce frequency broadening in the AS radiation only if the frequency of the vibrational coordinate x varies. This possibility could result from intermolecular interactions and will be discussed later. We examine first AS radiation produced by the second term in the dipole moment (5),

$$\mathfrak{y}''=(\partial\alpha/\partial x)\,bs\times\mathbf{E}. \quad (17)$$

The frequency broadening of the AS radiation from this term is due to the molecular rotation and the time variation of s. It is thus associated with Rayleigh scattering by the orientational Kerr effect. Using $\mathbf{E}=\mathbf{E}_0$ in (17) and for s and x the relations (8) and (13) derived for case (a) above, the average power transferred to the first AS field E_1' is

$$P_{E_1'}=-\tfrac{1}{8}(\partial\alpha/\partial x)\,bX_0\,|\,s_1'\,|\,|\,E_0\,|\,|\,E_1'\,|\,(\omega_0+\omega_M-\omega_R) \times\cos[(2\mathbf{K}_0-2\mathbf{K}_{-1}+\mathbf{K}_{-1}'-\mathbf{K}_1')\cdot\mathbf{r}+\psi], \quad (18)$$

with $\psi=2\phi_0-2\phi_{-1}+\phi_{-1}'-\phi_1'-\tan^{-1}\omega_R\tau$ for the case $\omega_1'=\omega_0+\omega_M-\omega_R$ and

$$P_{E_1'}=-\tfrac{1}{8}(\partial\alpha/\partial x)\,bX_0\,|\,s_1'\,|\,|\,E_0\,|\,|\,E_1'\,|(\omega_0+\omega_M+\omega_R) \times\cos[(2\mathbf{K}_0-\mathbf{K}_{-1}'-\mathbf{K}_1')\cdot\mathbf{r}+\psi], \quad (19)$$

with $\psi=2\phi_0-\phi_{-1}'-\phi_1'+\tan^{-1}\omega_R\tau$ for the case $\omega_1'=\omega_0+\omega_M+\omega_R$.

V. WAVE-VECTOR RELATIONS

The relations (18) and (19) give the wave-vector equations

$$2\mathbf{K}_0+\mathbf{K}_{-1}'=2\mathbf{K}_{-1}+\mathbf{K}_1', \quad (20)$$

$$2\mathbf{K}_0=\mathbf{K}_{-1}'+\mathbf{K}_1'. \quad (21)$$

From these the angles of emission of the first AS radiation may be derived. If the results from case (b) are used for s and x, the new wave-vector equations are

$$2\mathbf{K}_0=\mathbf{K}_{-1}'+2(\mathbf{K}_{-1}''-\mathbf{K}_{-1}''')+\mathbf{K}_1' \quad (22)$$

for $\omega_1'=\omega_0+\omega_M-\omega_R$, and again Eq. (21) for $\omega_1'=\omega_0+\omega_M+\omega_R$.

The difference between Eqs. (22) and (20) is clearer if we rewrite Eq. (20) in the form

$$2\mathbf{K}_0=\mathbf{K}_{-1}'+2(\mathbf{K}_{-1}-\mathbf{K}_{-1}')+\mathbf{K}_1',$$

which shows that (22) approaches (20) when $\omega_c\to\omega_M$.

The difference between (20) [or (22)] and (21) is simply due to the fact that the phase of s_1 containing $(\mathbf{K}_{-1}-\mathbf{K}_{-1}')$ [or $(\mathbf{K}_{-1}''-\mathbf{K}_{-1}''')$] enters twice in $P_{E'}$: with the same sign to generate $\omega_1'=\omega_0+\omega_M-\omega_R$ and with the opposite sign to generate $\omega_1'=\omega_0+\omega_M+\omega_R$.

Up to now, we have considered E_{-1}' on the low-frequency side of the Stokes spectrum, i.e., with $\omega_{-1}'=\omega_0-\omega_M-\omega_R$. If we consider E_{-1}' on the high-frequency side, i.e., $\omega_{-1}'=\omega_0-\omega_M+\omega_R$, it can be shown that (21) is obtained for $\omega_1'=\omega_0+\omega_M-\omega_R$ and (20) [or (22)] for $\omega_1'=\omega_0+\omega_M+\omega_R$. Since experiment shows clearly that the Stokes spectrum is much more intense on the low-frequency side, as expected from the pulse-steepening process, we limit our considerations to $\omega_{-1}'=\omega_0-\omega_M-\omega_R$.

Using in (17) a field E_1' with $\omega_1'=\omega_0+\omega_M-\omega_{R1}$, and proceeding in the same way, the field for the second AS radiation at a frequency $\omega_2'=\omega_0+2\omega_M-\omega_{R2}$ is generated. [See Fig. 4 for definitions of frequencies.] For it, the following wave-vector equations are obtained:

$$\mathbf{K}_0+\mathbf{K}_1'=\mathbf{K}_{-1}'+\mathbf{K}_2' \quad (23)$$

for the case $\omega_{R2}=\omega_{R2}'=\omega_{R1}-\omega_R$, and

$$\mathbf{K}_0+\mathbf{K}_1'+\mathbf{K}_{-1}'=2\mathbf{K}_{-1}+\mathbf{K}_2' \quad (24)$$

for $\omega_{R2}=\omega_{R2}''=\omega_{R1}+\omega_R$. Equations (23) and (24) have been derived using the results of case (a) for s and x. In case (b) the appropriate equation is

$$\mathbf{K}_0+\mathbf{K}_1'=\mathbf{K}_{-1}'+2(\mathbf{K}_{-1}''-\mathbf{K}_{-1}''')+\mathbf{K}_2', \quad (25)$$

which reduces to (24) when $\omega_c\to\omega_M$.

Similarly, for the third AS radiation, with a frequency $\omega_3'=\omega_0+3\omega_M-\omega_{R3}$ one obtains the following wave-vector equations:

$$\mathbf{K}_0+\mathbf{K}_2'=\mathbf{K}_{-1}'+\mathbf{K}_3' \quad (26)$$

for the case $\omega_{R3}=\omega_{R3}'=\omega_{R2}-\omega_R$, and

$$\mathbf{K}_0+\mathbf{K}_2'+\mathbf{K}_{-1}'=2\mathbf{K}_{-1}+\mathbf{K}_3' \quad (27a)$$

or

$$\mathbf{K}_0+\mathbf{K}_2'=\mathbf{K}_{-1}'+2(\mathbf{K}_{-1}''-\mathbf{K}_{-1}''')+\mathbf{K}_3' \quad (27b)$$

for $\omega_{R3}=\omega_{R3}''=\omega_{R2}+\omega_R$. Corresponding to the two different definitions of ω_{R2}, there are for ω_{R3} the definitions

$$\omega_{R3}'=\omega_{R1}-2\omega_R \quad\text{and}\quad \omega_{R3}'=\omega_{R1},$$

$$\omega_{R3}''=\omega_{R1} \quad\text{and}\quad \omega_{R3}''=\omega_{R1}+2\omega_R.$$

VI. MODULATION DUE TO MOLECULAR INTERACTIONS

In addition to molecular orientation, there is a second mechanism, mentioned briefly above, which can be responsible for frequency broadening in the Raman lines. It is the interaction between adjacent molecules in the liquid, which varies the molecular vibrational frequencies. A simple model of this process is described here. If the external field E induces dipole moments $\mathfrak{y}_1=\mathfrak{y}_2=\alpha\mathbf{E}$ on two more or less collinear adjacent molecules with a polarizability α, their mutual interaction energy is approximately

$$W_1=-2(\alpha^2E^2/d^3),$$

where d is the intermolecular distance. Since the field created by $\mathfrak{y}_1$ also induces a dipole moment

$$\mathfrak{y}_2'=-(2\mathfrak{y}_1/d^3)\alpha,$$

there is the additional coupling energy

$$W_2=-4(\alpha^3E^2/d^6).$$

This assumes that $W_2\ll W_1$, which is a gross approximation, but we are concerned here with obtaining only a rough magnitude for these effects. The total interaction energy from these terms gives a force

$$F=-\frac{\partial W}{\partial x}=4\frac{\alpha E^2}{d^3}\left(1+3\frac{\alpha}{d^3}\right)\frac{\partial\alpha}{\partial x}. \quad (28)$$

If x represents the amount of stretching of the molecule from the equilibrium value x_0, then $\alpha\simeq(x_0+x)^3\simeq d^3$, and we obtain an elastic force $F\simeq(10^2E^2x_0)x$ which opposes h_0x in Eq. (4). If $E=E_0\cos\omega_0t+E_0'\cos\omega_0't$ with $\Delta\omega=\omega_0-\omega_0'\ll\omega_0$ and $E_0\simeq E_0'$, we have $F=h_1(1+\cos\Delta\omega t)x$ with $h_1\simeq10^2E_0^2x_0$. This force produces a decrease in molecular frequency and a modulation of the frequency which is hence

$$\omega_M'\simeq\omega_M[1-\tfrac{1}{2}(h_1/h_0)][1-\tfrac{1}{2}(h_1/h_0)\cos\Delta\omega t]. \quad (29)$$

With the field obtainable inside the filaments, h_1/h_0 may be as large as a few percent.

As in the case of broadening by molecular orientational effects, the induced dipole moment may be taken for this second mechanism from (16) as

$$\mathfrak{y}'=(\partial\alpha/\partial x)\times\mathbf{E}.$$

This gives for the first AS the wave-vector equation

$$2\mathbf{K}_0=\mathbf{K}_{-1}'+\mathbf{K}_1', \quad (21')$$

formally identical to (21). The broad spectrum of E_1' is generated in this case by the different values of ω_{-1}' in the spectrum of E_{-1}'. Similarly, for the second AS radiation one obtains

$$\mathbf{K}_0+\mathbf{K}_1'=\mathbf{K}_{-1}'+\mathbf{K}_2', \quad (23')$$

formally identical with (23). Equation (23) gives the case $\omega_{R2}'=\omega_{R1}-\omega_R$ and (24) gives $\omega_{R2}''=\omega_{R1}+\omega_R$. However, Eq. (23') corresponds to the case ω_{R2}' when $\omega_{-1}'=\omega_0-\omega_M-\omega_R$ and to the case ω_{R2}'' when $\omega_{-1}'=\omega_0-\omega_M+\omega_R$. Because of the asymmetry in the intensity of the Stokes spectrum, the generation of ω_{R2}' is preferred to ω_{R2}''. For the third AS radiation the corresponding phase-matching equation is

$$\mathbf{K}_0+\mathbf{K}_2'=\mathbf{K}_{-1}'+\mathbf{K}_3', \quad (26')$$

which is formally identical with (26). The four possible values of ω_{R3} given by Eqs. (26) and (27) correspond in (26') to various positions of ω_{-1}' in the Stokes spectrum. Again because of the asymmetry of the Stokes spectrum, the strongest process corresponds to $\omega_{R3}'=\omega_{R1}-2\omega_R$ and the weakest to $\omega_{R3}''=\omega_{R1}+2\omega_R$.

VII. PHASE MATCHING AT A SURFACE, AND WAVEGUIDE EFFECTS

In order to derive from the above wave-vector equations the angular and spectral properties of the AS radiation, we must consider two other important consequences of the fact that the laser and Stokes light is trapped in filaments.

The first consequence is connected with the diameter d of the filaments. When $d\lesssim\lambda$, the transverse component of the wave vectors is undefined (or takes on a wide range of values) and only the matching of the components parallel to the axis of the filaments (z components) is meaningful in the wave-vector equations. The experimental value of d in the liquids examined is a few λ, and hence small enough to justify the approximation that only the z components need to be matched. This is similar to the requirement that phase matching need be done only at the surface parallel to the z axis.[16]

The second consequence is that the light propagates in a filament as in a dielectric waveguide. It may be shown[17] that even when the diameter of the guide is comparable to λ, the cutoff condition for a propagating mode is identical to the geometrical optics condition that the wave travels at an angle with respect to the axis which is the maximum allowed for total internal reflection.

Consider the simple model indicated by Fig. 5, of a cylindrical filament with refractive index $n+\Delta n$ in a medium of index n. The critical angle Θ_{cr}, corresponding to the trapping threshold, is given by

$$\cos\Theta_{cr}=[1+(\Delta n_{th}/n)]^{-1}\simeq1-(\Delta n_{th}/n), \quad (30)$$

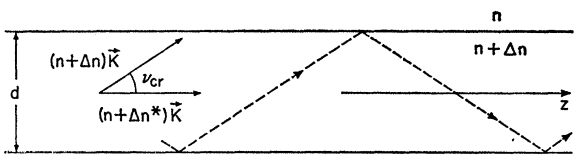

FIG. 5. Diagram for discussion of the waveguide effect in the filaments.

[16] A. Szöke, Bull. Am. Phys. Soc. 9, 490 (1964).
[17] E. Snitzer, J. Opt. Soc. Am. 51, 491 (1961).

where $\Delta n_{\rm th}$ is the threshold value for the increase in index within a filament which will trap light of angle $\Theta_{\rm cr}$. This is also just the angle for which the z component of the wave vector inside the filament is equal to that for a plane wave outside the filament traveling parallel to the z axis, since

$$K_z=[2\pi(n+\Delta n)/\lambda]\cos\Theta.$$

If the filament has an index of refraction greater than that necessary to trap a wave of a particular angle Θ with respect to the z axis, then the z component of the wave vector is

$$n\left(1+\frac{\Delta n}{n}\right)\cos\Theta K\simeq n\left(1+\frac{\Delta n-\Delta n_{\rm th}}{n}\right)K$$
$$=n\left(1+\frac{\Delta n^*}{n}\right)K. \quad (31)$$

Thus for this z component there is an effective difference in the index of refraction inside the filament, as compared with that of a plane wave outside the filament, of Δn^* given by the difference between the actual value of Δn and the threshold value for trapping $\Delta n_{\rm th}$.

VIII. EMISSION ANGLES

The angle of emission ϕ_1' of the first AS is now derived from the z component of Eq. (20),

$$2K_0+K_{-1}'=2K_{-1}+K_1'\cos\phi_1'. \quad (32)$$

Since the AS radiation emerges from the filaments, according to the refraction law K_{1z}' must have the same value inside and outside the filaments. Hence if K_1' is calculated outside the filaments, ϕ_1' represents the value of the emission angle in the liquid outside the filaments. Using the expansion

$$n=n_0+n'(\omega-\omega_0)+n''(\omega-\omega_0)^2 \quad (33)$$

for the dispersion, one obtains

$$\phi_1'^2=\frac{4}{n_1}\frac{\omega_M}{\omega_0+\omega_M}(\omega_M-2\omega_R)(n'+n''\omega_0)-2\left(\frac{\Delta n^*}{n}\right)_1 \quad (34)$$

to a first approximation in ω_R. The first term on the right-hand side is the square of the angle of emission inside the filament and Eq. (34) expresses Snell's law applied to obtain the angle of emission out of a filament with an effective index $n+\Delta n^*$. For the high-frequency side of the AS spectrum, Eq. (21) gives the continuation of Eq. (34). Using the more general Eq. (22) the following relation is derived:

$$\phi_1'^2=\frac{4}{n_1}\frac{\omega_M}{\omega_0+\omega_M}\left(\omega_M-2\frac{\omega_c}{\omega_M}\omega_R\right)(n'+n''\omega_0)-2\left(\frac{\Delta n^*}{n}\right)_1. \quad (34')$$

This reduces to (34) when $\omega_c\rightarrow\omega_M$.

For the second AS radiation, Eq. (23) gives

$$\phi_2'^2=4\frac{[3\omega_M(\omega_M-\omega_{R2}')-\omega_{R1}\omega_{R2}'](n'+n''\omega_0)}{n_2(\omega_0+2\omega_M)}$$
$$-2\left(\frac{\Delta n^*}{n}\right)_2 \quad (35)$$

and Eq. (24) gives

$$\psi_2'^2=4\frac{[3\omega_M(\omega_M-\omega_{R2}'')+\omega_R\omega_{R2}''-\omega_R^2](n'+n''\omega_0)}{n_2(\omega_0+2\omega_M)}$$
$$-2\left(\frac{\Delta n^*}{n}\right)_2. \quad (36)$$

Equation (23′) gives (35) for the case $\omega_{R2}=\omega_{R2}'$ and (36) (without the term ω_R^2) for $\omega_{R2}=\omega_{R2}''$. Both (35) and (36) are derived with the approximation $\omega_M/\omega_0\ll1$ in the coefficient of n'', and using for ϕ_1' the expression derived from (20).

Angles of emission for the third AS radiation may be obtained from Eqs. (26), (27), and (26′), with approximation of the same order as

$$\phi_3'^2=8\frac{\omega_M(3\omega_M-2\omega_{R3})(n'+n''\omega_0)}{n_3(\omega_0+3\omega_M)}-2\left(\frac{\Delta n^*}{n}\right)_3 \quad (37)$$

for each of the possible definitions of ω_{R3}.

It should be emphasized that in the above, the frequencies ω_R are assumed to be considerably larger than what would be produced by a single stimulated Rayleigh process. Such might be the result, for example, of multiple Rayleigh processes or of nonlinear propagation of an intensity modulated wave or pulse.[10,12,13]

IX. COMPARISON WITH EXPERIMENTAL RESULTS

The experimental results shown in Fig. 2 may now be interpreted on the basis of Eqs. (34) to (37). The surface-matching conditions for the wave vectors of the interacting waves produce AS emission with angles, inside the filaments, which are parabolic functions of frequency ω_{Ri} [first term in the right-hand side of Eqs. (34) to (37)]. Since the radiation is generated inside a number of filaments with various values of Δn^*, a more-or-less continuous spectrum of values of the emission angles out of the filaments is expected at a fixed frequency. However, a single filament produces a parabolic distribution, according to (34), and when there are only a few strong filaments, then the main intensity occurs along a few nested parabolas and the distribution at a fixed frequency corresponds to a few discrete angles. When, at a given frequency, the angle of emission inside the filament is less than

$$(2\Delta n^*/n)^{1/2},$$

the radiation is trapped and may be converted to another frequency by the many nonlinear processes

TABLE I. Values of $\Delta n^*/n$ for which Eqs. (34) to (37) describe the most intense part of the spectra. The values of

$$\tfrac{1}{2}(\phi_{1\,\mathrm{int}}^2) \quad \text{and} \quad \tfrac{1}{2}(\phi_{2\,\mathrm{int}}^2),$$

which give another value of $\Delta n^*/n$ from Eqs. (39) and (40), are also listed.

Liquid	$10^4\times(\Delta n^*/n)_1$	$10^4\times(\Delta n^*/n)_2$; internal	$10^4\times\frac{1}{2}(\phi_{1\,\mathrm{int}}^2)$ external		$10^4\times(\Delta n^*/n)_3$; internal	$10^4\times\frac{1}{2}(\phi_{2\,\mathrm{int}}^2)$ external	
Benzene	1.30	2.35	5.20	3.70	3.60	6.80	10.2
Carbon disulfide	1.38	5	...	3.45	6.90	11.90	9.85
Toluene	3.25	8	10.45	5	11.75	15.90	15
Nitrobenzene	4.80	11.50	20	11.90	...	...	

occurring in the filaments. It may be seen from Eqs. (34), (35), and (37) that the processes considered can shift the frequency downward by a maximum of $\omega_{M/2}$, ω_M, $3/2\omega_M$ for the first, second, and third AS, respectively. These results hold only in the absence of further shifts due to pulse steepening or phase modulation of the AS radiation, which will be shown below to be unlikely.

The fact that the first AS spectrum is predominantly shifted to the low-frequency side may be explained by a shift of the central frequency $\omega_0+\omega_M$ due to a decrease either of ω_M, according to Eq. (29), or of ω_0 due to pulse steepening of the laser light. To compare Eq. (34) with the experimental results we use a value of $(\Delta n^*/n)_1$ such that ϕ_1' agrees with the corresponding experimental value at a given frequency. The profile of the spectrum is then compared with Eq. (34). Since the first AS exhibits a broadening less than $\simeq$0.10–0.12 ω_M without evidence of single well-defined parabolas, the comparison is restricted to a limited range of values of ϕ_1' and ω_{R1}. The dispersion coefficients n' and n'' are calculated for carbon disulfide, benzene, and nitrobenzene from Ref. 18 and those for toluene from Ref. 19.

The agreement between Eq. (34) and the experimental results is satisfactory for carbon disulfide and toluene, while Eq. (34′) rather than (34) is needed to fit the experimental results for benzene. Note that according to Eq. (34) the emission angle at a given frequency $\bar{\omega}_R$ depends only on Δn^*, and filaments with the same Δn^* produce AS emission described by the same parabola. According to Eq. (34′), filaments with the same Δn^* give the same emission angle at $\omega_R=0$, but different angles at any $\omega_R=\bar{\omega}_R$, depending on the value of

$$\omega_c/\omega_M.$$

Because of the increasing frequency shift of the Stokes spectrum due to the self-steepening process,[12] the difference between the spectra described by Eqs. (34) and (34′) increases with the path length of the optical pulse. Since ω_c/ω_M increases with this path length, it is expected that a filament with a fixed Δn^* produces AS emission described by parabolas with the apex approaching ω_1 as the filament proceeds in the liquid, generating in this way a broad spectrum. The same process can occur also in the higher-order AS emission, although analytically described by equations more complicated than (34′). Experimentally there is in fact evidence of parabolas giving the same angle at "zero-frequency broadening" but crossing the $\phi=0$ axis at different points, especially for CS_2 in the third AS, as may be seen in Fig. 2.

Two different families of cones are predicted for the second anti-Stokes from Eqs. (35) and (36), which assume a frequency $\omega_1'=\omega_0+\omega_M-\omega_{R1}$ for the first AS. The existence of two distinct cones of emission is experimentally found for toluene, benzene, and nitrobenzene, but not for carbon disulfide. The "external" cone, corresponding to the larger emission angle, exhibits a frequency broadening both to the low- and high-frequency side and is described by Eq. (35), in which $\omega_{R2}'=\omega_{R1}-\omega_R$ may be either positive or negative. The "internal" cone presents a broadening predominately to the low-frequency side and is described by Eq. (36) with $\omega_{R2}''=\omega_{R1}+\omega_R$, which may be only positive. Equations (35) and (36) fit the experimental spectra in a satisfactory way for all the liquids in the sense that with the values of Δn^* which give the experimental value of the inner and outer cone angles, ϕ_2 and ψ_2, at $\omega_{R2}=0$, the entire profiles of the spectra are reproduced with deviations of only a few percent. Representative values of Δn^* are given in Table I. To describe angles smaller in one cone than in the other, Eqs. (35) and (36) require separate values of Δn^* which may differ by as much as a factor of 2. This difference may be understood by considering the asymmetry of the Stokes spectrum due to self-steepening. Equation (35), being derived from Eq. (23′) with $\mathbf{K}_{-1}'$ in the most intense part of the Stokes spectrum, represents the most intense emission cone. Its production requires a field strength (and consequently a Δn^*) smaller than that required for the cone given by Eq. (36).

Similar considerations apply to the third AS radiation.

[18] V. G. Cooper and A. D. May, Appl. Phys. Letters **7**, 74 (1965).

[19] International Critical Tables (McGraw-Hill Book Co., New York, 1930).

Here also two different cones of emission are evident for toluene, benzene, and carbon disulfide, while for nitrobenzene there is no evidence of emission of the third AS. Equation (37), with $\omega_{R3}'=\omega_{R1}-2\omega_R$, represents the "external" and most intense emission cone, while with $\omega_{R3}'=\omega_{R1}$ or $\omega_{R3}''=\omega_{R1}+2\omega_R$ it represents the weaker internal cone. Assuming two values of Δn^*, different for the same reason mentioned above, a satisfactory fitting of the experimental profiles is found also for Eq. (37).

While trapped radiation often exhibits discrete spectra[9,10] and, occasionally, a very well-defined semi-periodic structure, untrapped AS radiation seems to present a continuous frequency broadening. This may be due to the fact that the AS radiation collected in the far field is formed by the superposition of different contributions. These contributions are generated along the path length of the filaments by trapped radiation with a discrete spectrum which continuously shifts in frequency or intensity distribution as the filaments proceed in the liquid.[12,13]

X. ANTI-STOKES RADIATION ALONG THE FILAMENT AXIS

The angles of AS emission, given by Eqs. (34) to (37), may be written in the general form

$$\phi_i'^2=\phi_{i\ \mathrm{int.}}'^2(\omega_{Ri})-2(\Delta n^*/n)_i. \tag{38}$$

As Δn^* in (38) increases, the emission angle ϕ_1' for a given frequency ω_{Ri} decreases until, for $2(\Delta n^*/n)_i$ equal to $\phi_{i\ \mathrm{int.}}^2$ (0), all of the AS radiation generated in the filament is trapped. Since the second AS is generated by modulation of the first AS, we expect to find the maximum of intensity of the second AS from those filaments in which the first AS is completely trapped, i.e., with Δn^* given by

$$\phi_{1\ \mathrm{int.}}^2(\omega_{R1}=0)\lesssim 2(\Delta n^*/n)_2, \tag{39}$$

and similarly for the third AS

$$\phi_{2\ \mathrm{int}}^2(\omega_{R2}=0)\lesssim 2(\Delta n^*/n)_3. \tag{40}$$

The values of $(\Delta n^*/n)$ for which Eqs. (34) to (37) describe the most intense part of the spectra are indicated in Table I. These values are consistent with those given by (39) and (40), which are also listed in Table I.

FIG. 6. Spectra of single filaments in carbon disulfide. The picture is obtained by imaging the end of the cell on the open slit of the spectrometer. The laser line is indicated by L, the first AS by AS_1 and the first Stokes by S_1. The picture does not accurately represent relative intensities of the lines.

One may wonder whether nonlinear pulse propagation affects directly the AS spectra. Generally the AS radiation observed at an angle in the far field has been inside a filament for too short a distance to be much affected by pulse steepening or phase modulation, since the reflection coefficient at the boundary of a filament decreases rapidly as $\phi_{i\ \mathrm{int.}}'$ increases above

$$(2\Delta n^*/n)^{1/2}.$$

The reflection coefficient is less than 10% for

$$\frac{\phi_{i\ \mathrm{int.}}'}{(2\Delta n^*/n)^{1/2}}\geq 1.2.$$

However, radiation traveling in a filament near the limiting angle for trapping remains inside the filament for a longer distance and is much more subject to nonlinear pulse propagation effects. This radiation emerges almost parallel to the filament itself and is particularly intense because of the increased interaction distance in the filament. In the far field pattern this should produce a bright spot or line corresponding to angles $\phi_i'\approx 0$. This phenomenon is in fact frequently seen. It is illustrated in the first AS radiation of Figs. 2(a) and 2(b), and in the first and second AS spectra of Fig. 2(c). In the latter case, a line appears at $\phi_i'\approx 0$, corresponding to considerable frequency broadening. This may be due to pulse steepening and phase modulation.

The AS radiation which is completely trapped in filaments may undergo considerable frequency broadening due to nonlinear pulse propagation, which should give most pronounced broadening on the low-frequency side of the unshifted AS frequency. Near-field observations of the AS frequency do in fact confirm the existence of filaments with approximately the same frequency broadening as the Stokes radiation. This is illustrated in the carbon disulfide spectrum of Fig. 6.

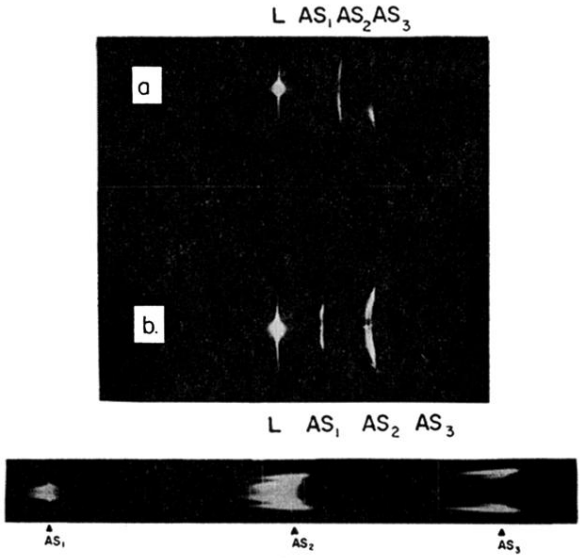

(c)

FIG. 2. Typical patterns of AS-radiation, with frequency increasing from left to right, and angle of the radiation measured up or down from the symmetry axis, which corresponds to the direction of the laser light. Frequency separation between AS orders (AS_1, AS_2, AS_3) corresponds to the molecular vibrational frequency of a few hundred wave numbers. Maximum angle deviations in these figures are about $\pm 5°$. Spectra shown are for (a) carbon disulfide, (b) benzene, and (c) toluene. Because of varying spectral sensitivity of the film (Polaroid 57) and the filters used (Corning glass 4-97), the pictures do not accurately represent the relative intensities of the laser frequency and different AS orders.

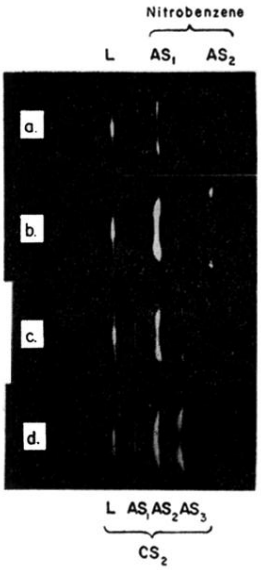

FIG. 3. Examples of AS-spectra in a mixture of nitrobenzene and carbon disulfide. The frequency broadening of the AS lines depends on the relative concentration of the two liquids. (a) Pure nitrobenzene, (b) mixture with 40% (volume) CS_2, (c) mixture with 45% (volume) CS_2, (d) mixture with 66% (volume) CS_2.

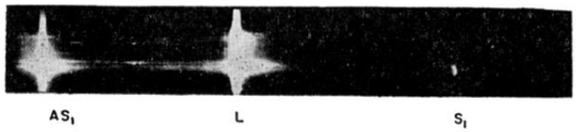

FIG. 6. Spectra of single filaments in carbon disulfide. The picture is obtained by imaging the end of the cell on the open slit of the spectrometer. The laser line is indicated by L, the first AS by AS_1 and the first Stokes by S_1. The picture does not accurately represent relative intensities of the lines.